ELSEVIER

Ultramicroscopy 84 (2000) 149–157

ultramicroscopy

www.elsevier.nl/locate/ultramic

Near-field scanning optical microscopy of zinc-porphyrin crystals

Robert Brunner[a,1], Margaret E. Kosal[b], Kenneth S. Suslick[b], Ralf Lamche[c], Othmar Marti[c], Jeffrey O. White[a,*]

[a] *Frederick Seitz Materials Research Laboratory, University of Illinois, 104 S. Goodwin Avenue Urbana, IL 61801, USA*
[b] *School of Chemical Sciences, University of Illinois, Urbana, IL, USA*
[c] *Department of Experimental Physics, University of Ulm, Ulm, Germany*

Received 27 July 1999; received in revised form 17 January 2000

Abstract

Using a near-field scanning optical microscope (NSOM), crystals of zinc-porphyrin network materials are characterized with respect to morphology and fluorescence. Needle-shaped crystals are observed. While the topography is flat, the fluorescence intensity profile in the width direction is approximately triangular. A numerical calculation shows that differences between the topographic and optical images cannot be due to an artifact. In some needle-shaped crystals, the fluorescence emission is strongly peaked at one or both ends, possibly indicating a polar crystal structure.

PACS: 42.70.Jk; 07.79.F; 78.55.M; 78.55.K

Keywords: Scanning near-field optical microscopy; Microscopic examination of materials; Organic crystals; Fluorescence

1. Introduction

Porphyrins are of enormous importance to the functioning of biological systems. To gain an understanding of the catalytic properties of natural porphyrins, their physical structure has been thoroughly studied. There have also been attempts to synthetically mimic and control the catalytic properties [1]. We have been exploring nanoporous metallo-porphyrin crystalline solids as possible size- and shape-selective oxidation catalysts. Zinc–porphyrin-doped PMMA has also recently been used as a photochromic recording medium [2].

Under different growth conditions, the porphyrin molecules crystallize in a wide variety of shapes, for example, needles, plates, cubes or hexagons. One reason to optimize the growth parameters is to obtain samples large enough to analyze with X-ray diffraction. The present state-of-the art in growth techniques yields crystals from 0.1 to 10 μm in size, an appropriate length scale for

*Corresponding author. Tel.: +1-217-333-8876; fax: +1-217-244-2278.

E-mail address: white5@uiuc.edu (J.O. White).

[1] Current address: Carl Zeiss Jena GmbH, D-07740 Jena, Germany

0304-3991/00/$ - see front matter
PII: S0304-3991(00)00027-9

characterization by scanning probe microscopy. In particular, near-field scanning optical microscopy (NSOM) offers the possibility to measure simultaneously the topography and the optical properties of a sample, well below the lateral classical resolution limit [3]. Near-field optical microscopy has already been used to study wheel-shaped porphyrin crystals [4].

Near-field microscopy involves scanning a subwavelength aperture over a sample, at a height of 5–20 nm, and building up the image point by point. In many samples, it is advantageous to excite the sample with one wavelength and collect the fluorescence at another wavelength. When using tapered and aluminized glass fiber tips as near-field probes [5], the distance control between tip and sample is usually done by the shear-force technique [6,7]. The fiber tip is excited at a mechanical resonance, typically in the 10–100 kHz range. At tip heights <20 nm, the oscillation is damped due to surface interactions. Using the damping as a feedback signal allows the tip-surface distance to be controlled in the subnanometer range, using piezoelectric transducers. The signal applied to the transducers therefore furnishes a topographic image recorded in parallel with the optical image.

In this paper we present the results of NSOM investigations of coordination networks of the Zn(II) derivative of meso-*tetrakis*-(4-carboxy)tetraphenyl porphyrin, Zn(p-COO)TPP. The zinc–porphyrin molecular building blocks possess four symmetrical carboxylic acid substituents. When deprotonated, these carboxylic acid groups can coordinate to metals ions forming one, two or three-dimensional polymers. When excited with light, the zinc-porphyrin crystals fluoresce with high efficiency.

One unusual feature is that the fluorescence at the crystal ends is frequently much stronger than at the center, with no corresponding feature in topography. The fluorescence and topography crossections in width are also different. The topographical crossection shows steep edges at the sides of a broad, flat plateau. In contrast, the fluorescence crossection is roughly triangular. We discuss in detail the origin of these differences, because they relate to image fidelity. In particular, the absence of differences, i.e., too strong a correlation between the two images, is a sign of cross-talk between the topographic and optical images.

2. Experimental procedure

A schematic of the NSOM[2] is shown in Fig. 1a. In fluorescence transmission mode, the light emitted by the probe interacts with the sample and is collected by a high numerical aperture microscope objective. The microscope objective focuses the light onto the active area of an avalanche photodiode (APD). Due to the small active area of the detector compared to the image of the tip, a confocal system is realized. A colored glass filter blocks the excitation light and transmits the fluorescence. To reduce topography-induced artifacts, only the sample is translated during the scan; all of the optics remain stationary.

The sample is translated by a piezoelectric stage with capacitive position sensing, a range of $100\times100\times10\,\mu m^3$, and a lateral resolution of 1 nm. Fluorescence is excited with the 514.5 nm line of an argon-ion laser. To reduce stray light effects which may disturb the optical signal, the distance control is done by a non-optical shear-force detection system [8].

Tapered and aluminized glass fiber tips are prepared in the conventional way [5]. The essential optical and mechanical characteristics of the fiber tips are tested prior to use. First, the tip is examined with a microscope to assure the absence of unintentional pinholes. Via scanning electron microscopy, some apertures were found to be $\sim$100 nm in diameter (Fig. 1b). The aperture size of the other tips was estimated using the optical throughput. The vibrational amplitude of the tips is kept in the range of 10 nm, so as not to affect the resolution.

The zinc–porphyrin crystals were prepared via hydrothermal synthesis. A stoichiometric excess of a zinc salt and unmetallated porphyrin starting

[2] Witec Alpha-SNOM, Wissenschaftliche Instrumente und Technologie GmbH, Albert Einstein Allee 15, 89091 Ulm, Germany.

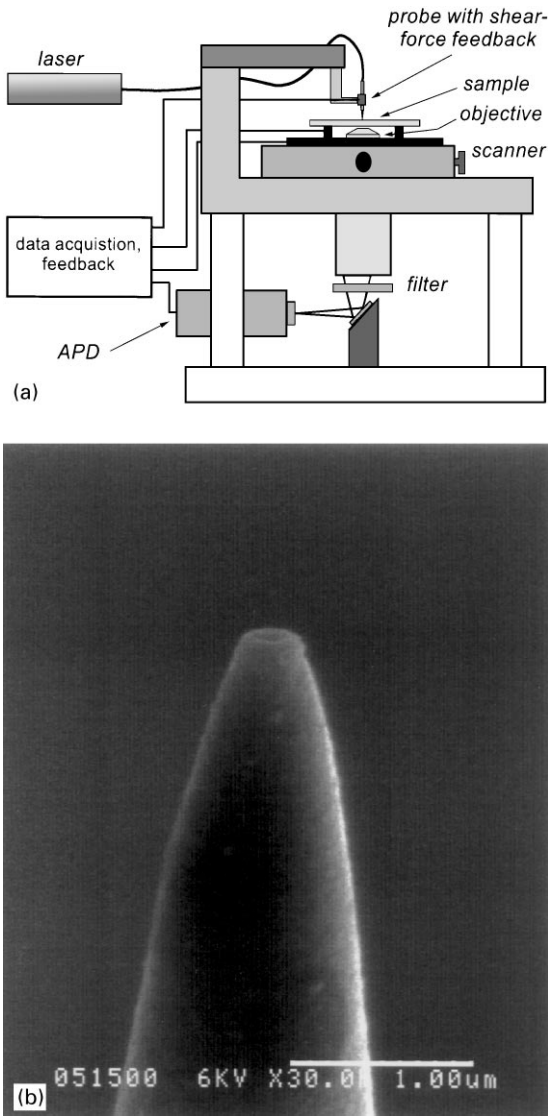

Fig. 1. (a) Schematic view of the NSOM setup. The light emitted by the fiber probe excites fluorescence, which is focused on the avalanche photodiode. A band pass filter separates the excitation and fluorescence light. To reduce topography-induced artifacts in the optical image, the sample is scanned rather than the probe. The tip–surface distance control is done by piezoelectric shear-force feedback. (b) SEM image of a fiber tip.

material were dissolved in basic water and heated in a closed pressure reactor. After heating to temperatures above 100°C for a specific time period (12–96 h), the materials were subject to slow cooling. Three zinc salts were used: the nitrate, acetate, and hydrated chloride. Similar morphologies were observed with all three.

3. Results and dicussion

Fig. 2 shows topographic and fluorescence images of a large ($25\times25\,\mu m^2$) region of the sample. The rod-like zinc-porphyrin crystals have length, width, and height in the range 1–15, 0.1–1.5, and 0.4–0.5 μm. A conspicuous difference between the two images is that the porphyrin crystals appear narrower in fluorescence, i.e., the optical and topographical width crossections are quite different. The topography has a flat, ~1 μm plateau, bounded by sharp edges. In contrast, the fluorescence increases linearly over a distance of ~500 nm, reaching a maximum in the center of the structure.

For a more detailed view, the scan was repeated on a $5\times5\,\mu m^2$ region (Fig. 3). In these images as well, the fluorescence evidently has a spatial dependence quite distinct from the topography. The topographic width crossections of a second porphyrin crystal also show a flat topography and a peaked fluorescence.

Both topographic and optical images are influenced by a combination of probe and sample properties. This effect can yield a better lateral resolution in fluorescence than in topography, and was observed on wheel-shaped porphyrin crystals [4]. The real topography can be estimated by a deconvolution of the measured topography and the probe geometry. This particular probe had a flat tip with a diameter of 270 nm. The aperture was ~120 nm in diameter and the aluminum coating had a thickness of ~75 nm. Three hundred nanometers above the aperture, the probe diameter was already ~500 nm. According to the topographic image, the edges of the plateau have a slope between 25° and 30°, which corresponds very well to the taper angle of the tip. That means that the true slope is actually steeper, and also that the true plateau width is about 270 nm less than the measured value of ~1 μm.

It has been shown that there is a high risk of topography-induced artifacts in NSOM images [9].

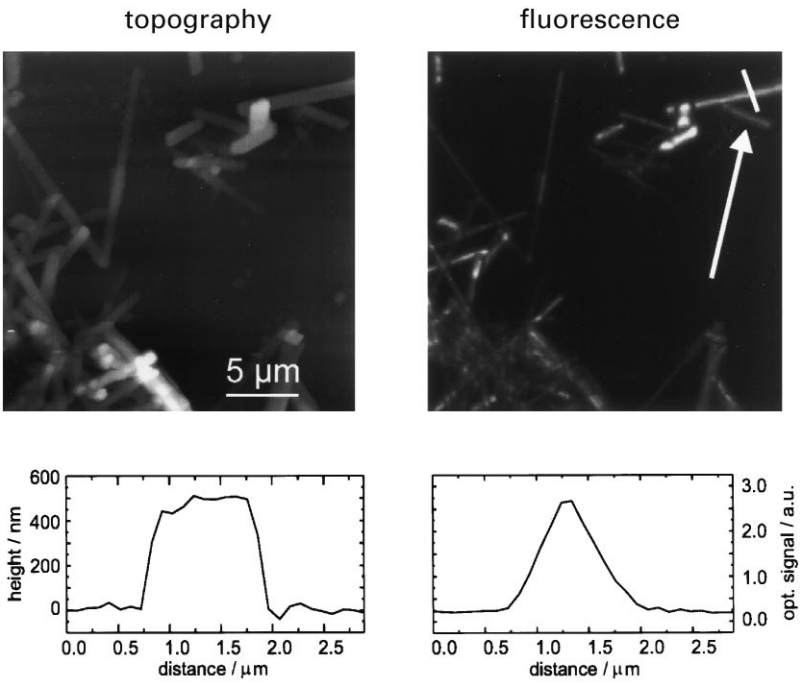

Fig. 2. Topographic and fluorescence overview of porphyrin crystals dispersed on a glass substrate. The needle-shaped crystals are 1–15 µm in length. The width crossection (white bar in the upper right corner) shows a different shape in topography and fluorescence.

Reliable near-field optical images should either be uncorrelated to the topography, or the correlated structures in both images should be displaced by a constant amount, or the resolution in topography and optical image should be different. Even when these criteria are met, NSOM images can be difficult to interpret. Measuring fluorescence, rather than simple transmission or reflection, also minimizes the possibility of artifacts [10].

To determine the real fluorescence profile of the porphyrin crystals, it is necessary to deconvolve the optic image. Due to the complex field distribution emitted by the aperture and penetrating into the surface, it is more difficult to deconvolve the fluorescence image than the topographic image. Although the electromagnetic field emitted by the aperture decays rapidly, the fluorescence is excited inside the crystal and not only at the surface. Numerical calculations of the field distribution of near-field probes show that, at a distance below the aperture comparable to its diameter (120 nm in our case), the on-axis intensity is reduced to a few percent relative to the value at the aperture [11]. Therefore, objects such as ours, which are several 100 nm thick, cannot be considered infinitesimally thin, and one needs at least a two-dimensional calculation.

During a scan, the radiation emitted by the aperture is not a constant but depends on the optical properties and morphology of the sample. For example, simulations predict a repulsion of the electric field in the presence of metals and an attraction toward dielectric objects [12,13]. During scanning, when the aperture starts to overlap with the top of the crystal, the radiation begins to penetrate into the crystal and the fluorescence signal increases. Due to the attraction of the electric field towards the dielectric porphyrin, the fluorescence should rapidly increase as the aperture moves across the edge of the crystal. Assuming spatially uniform fluorescence efficiency in the crystal, the emission is expected to be nearly at its maximum as soon as the whole aperture overlaps the crystal. It should stay approximately constant

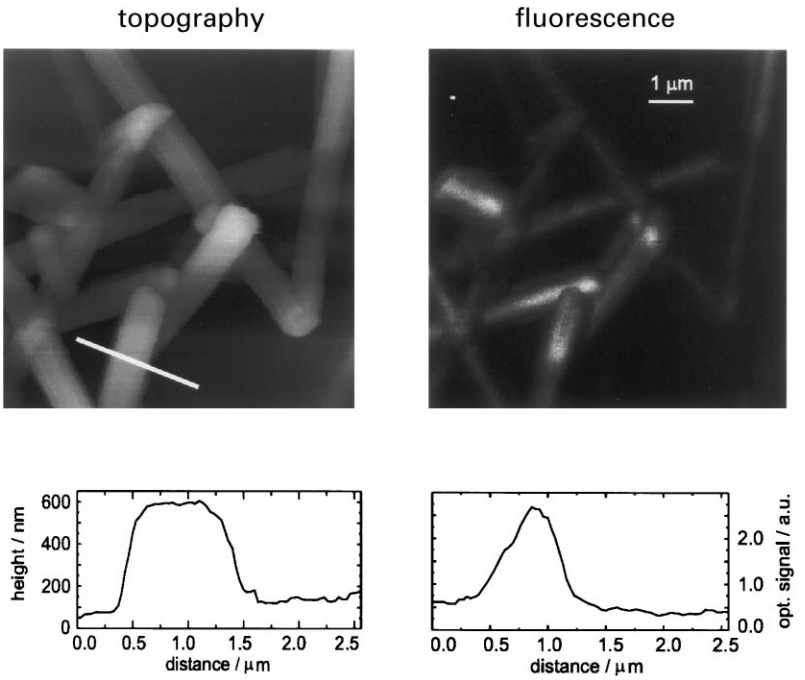

Fig. 3. Detailed view of the region left of center in Fig. 2. Also on this scale the difference between the topographic and fluorescence images becomes obvious. The crossection (white bar) in the topography show a flat plateau surrounded by sharp edges, whereas the fluorescence intensity is peaked in the center of the rod.

until the tip reaches the opposite side of the crystal.

The expected flat plateau in the fluorescence was not observed in our experiments. All crystals showed a clear central peak. For example, the crossection of the crystal in Fig. 2 shows a fluorescence intensity that increases over a distance of 500 nm. Although this length is more than four times the aperture diameter, qualitative arguments alone cannot exclude the possibility that the measured signal is an artifact of tip geometry.

To verify that the increased fluorescence in the center of the porphyrin is not an experimental artifact, a numerical calculation was performed with the electromagnetic simulation software (MAFIA Maxwell's Equations by Finite Integration Algorithm). It has already been shown that MAFIA is an appropriate software tool for near-field simulations [14]. In particular, the results based on MAFIA are in excellent agreement with the well-established multiple multipole method (MMP) [12].

Fig. 4 shows the electrical field energy density calculated in a two-dimensional model, for four positions of the probe. The porphyrin crystal was described by a rectangle of uniform fluorescence efficiency, refractive index 1.55, height 400 nm, and width 800 nm (see crossection of Fig. 2). The tip aperture diameter was set to 120 nm, the surrounding metal coating had a thickness of 75 nm and the excitation wavelength was 514.5 nm. At each position of the probe, the emitted fluorescence is estimated by integrating the field energy density inside the crystal.

In the first plot (Fig. 4a), only half of the aperture covers the crystal, but more than 80% of the energy emitted by the probe is inside the crystal (relative to Fig. 4d). In the second plot (Fig. 4b), the whole aperture is inside the edge of the crystal, and already more than 90% of the energy is inside the crystal. With the aperture 130 nm across the crystal (Fig. 4c), 96% of the energy is inside the crystal. The maximum (100%) is reached at the position where the probe is at the center (Fig. 4d).

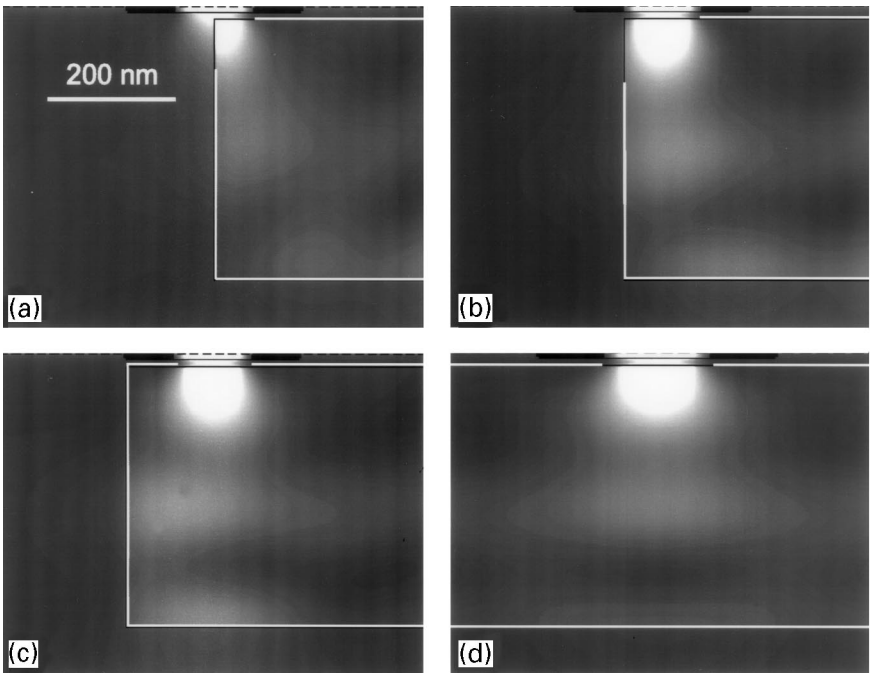

Fig. 4. Electrical field energy density calculated for four positions of the tip relative to the sample (white outline). (a) The center of the aperture is above the sample edge. (b) The entire aperture is above the sample. (c) The center of the aperture is 130 nm from the sample edge. (d) The tip is centered over the sample. In (a), the energy density inside the crystal is 80% relative to (d). In (b) and (c) the corresponding values are 90% and 96%.

The triangular fluorescence crossection seen in our experiments is incompatible with this simulation. This verifies that the strongly peaked fluorescence in the experimental images is not an artifact.

Fig. 5 shows that enhanced fluorescence at the crystal extremities is also observable in regions of the sample where the rods are close together or overlapping. This effect cannot be explained by a simple tip–sample convolution, either, because the ends of the rods show no apparent change in topography. Fig. 6 shows a better example. The length crossection is flat in topography, but has a sharp peak in fluorescence. The peak has intensity 2.5× higher than the rest of the crystal. Only one end shows the pronounced fluorescence. Fig. 7, a combination of several scans, shows a large crystal with a length of about 13.5 μm.[3] At the lower end, the fluorescence clearly increases. The smaller rod in the lower image shows an increased fluorescence at both ends. The fluorescence from the rod ends is about 1.6× more intense compared to the center.

A possible explanation for the intense fluorescence at the crystal ends is multiple Förster energy transfer. The emission from molecules excited in the central regions of the crystal is reduced by the possibility that the excitation can escape essentially in two directions. At the crystal ends, the excitation can escape in only one direction (toward the center), therefore the emission should be enhanced. In this case, however, an enhanced fluorescence should always be seen in both ends of the crystal, contrary to our observations.

Another possible explanation would be a change of crystal composition or structure, which simultaneously enhances the fluorescence and stops the growth along the long axis. That would

[3] In comparison to a tube scanner, a capacitively-controlled scan table allows us to overcome the problem of piezo nonlinearities and also allows an exact selection of scan range.

Fig. 6. The crossection along the length of the crystal is flat, but the fluorescence profile has a sharp peak at one end. The peak has intensity 2.5× that of the rest of the crystal.

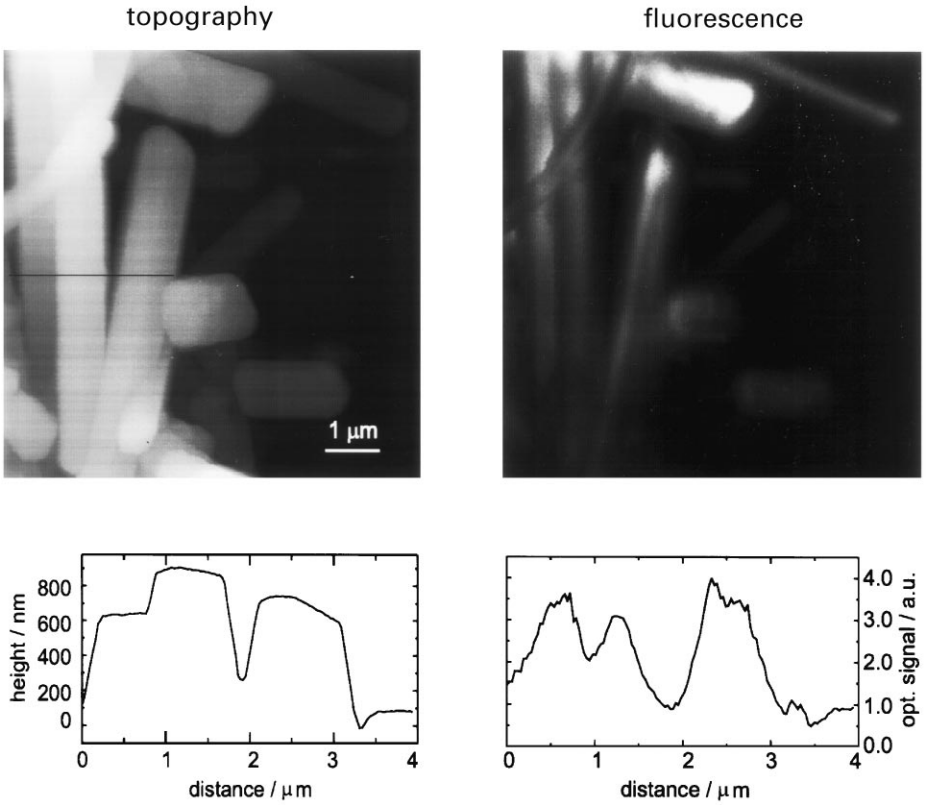

Fig. 5. Rods showing an increased fluorescence at the ends, with no apparent change in topography.

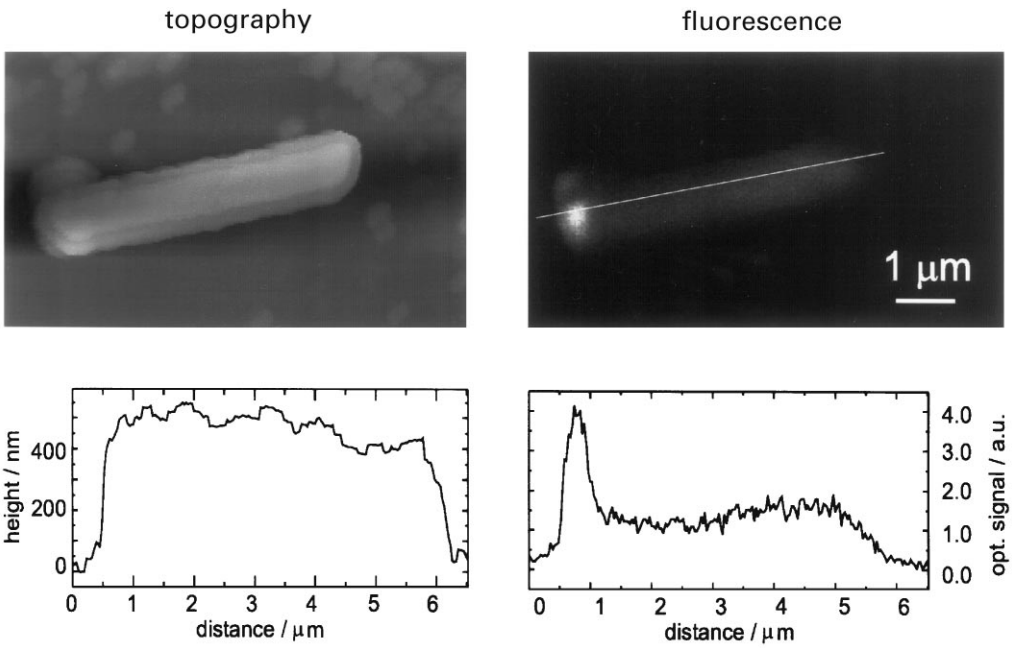

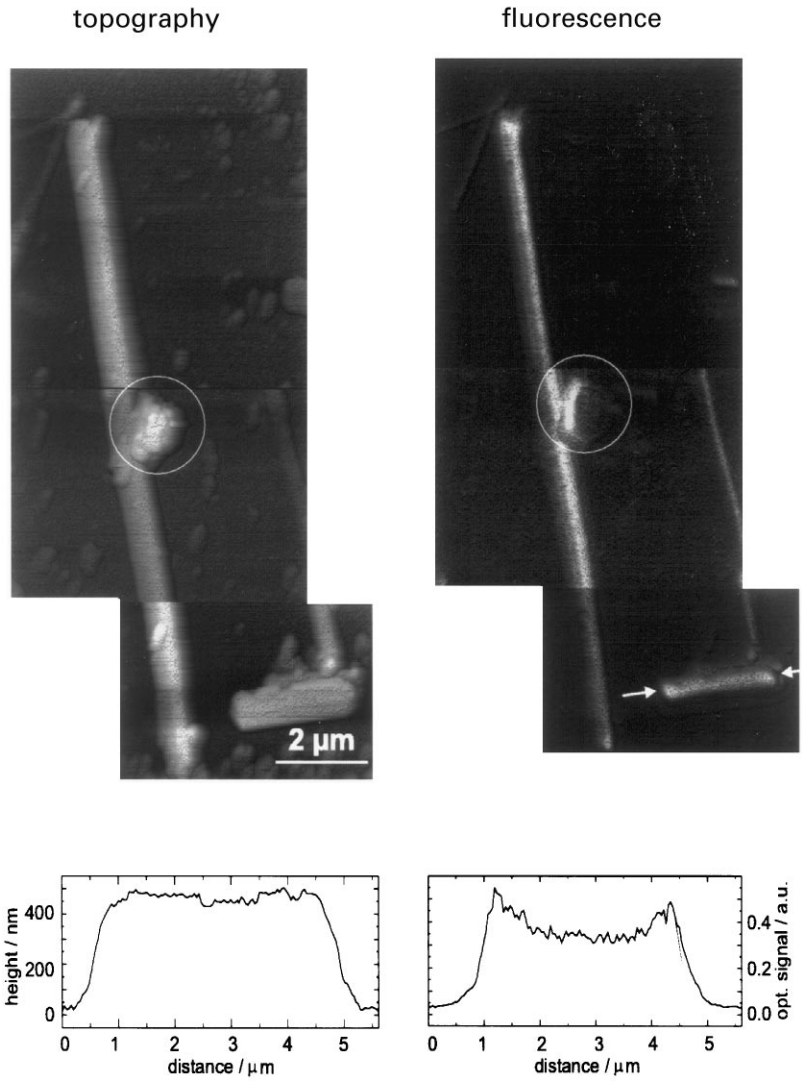

Fig. 7. Composite of three scans. The nonfluorescent structures may be sodium salts that precipitate during sample preparation. Fluorescence peaks are present at the ends of the small porphyrin crystal in the lower image.

explain why a fluorescence increase is only observed at the ends of the rod. When the enhancement is not observed, presumably there is no alteration of composition or structure. It seems unlikely, however, that changes in crystal composition or structure would lead only to increases, and never decreases in fluorescence.

As another sign that cross-talk is not a problem in our images, some structures appear in topography but not fluorescence (Fig. 7). These structures may be solid sodium salts that precipitate as the aqueous solvent evaporates during air drying of the microscope slides.

4. Conclusions

NSOM has been used to study simultaneously the topography and fluorescence of needle-shaped zinc–porphyrin crystals. Width crossections were flat in topography and peaked in fluorescence. Further analysis shows that the fluorescence peak

in the crystal center is not an artifact. A qualitative deconvolution to allow for the affect of the tip geometry suggests that the fluorescence peak is real. A two-dimensional numerical simulation of the experiment confirms this result.

Several rod-like porphyrin crystals also displayed an enhanced fluorescence at the rod ends, with no corresponding topographical feature. The enhancement occurred at one or both ends of the crystal. The origin of this effect is still unclear.

Acknowledgements

This work was funded by the US Department of Energy, Division of Materials Science Grant DEFG 02-96ER45439 and by the German Ministry of Science and Technology (BMBF), grants 13N/6522 and 13N/7040. Near-field measurements were made in the Materials Research Laboratory Laser Facility. We are also indebted to Dr. Joachim Koenen of Witec GmbH for many helpful discussions.

References

[1] K. Suslick, S. van Deusen-Jeffries, in: J.-M. Lehn (Ed.), Comprehensive Supramolecular Chemistry, Vol 5. Bioinorganic Systems, K. Suslick (Ed.), Elsevier Science, Oxford, 1996, pp. 1–30.

[2] O.V. Khodykin, S.J. Zilker, D. Haarer, B.M. Kharlamov, Opt. Lett. 24 (1999) 513.

[3] M.A. Paesler, P.J. Moyer, Near-field Optics Theory, Instrumentation and Applications, Wiley, New York, 1996.

[4] J. Hofkens et al., J. Phys. Chem. B 101 (1997) 10588.

[5] G.A.. Valaskovic, M. Holton, G.H. Morrison, Appl. Opt. 34 (1995) 1215.

[6] R. Toledo-Crow, P.C. Yang, Y. Chen, M. Vaez-Iravani, Appl. Phys. Lett. 60 (1992) 2957.

[7] E. Betzig, P.L. Finn, J.S. Weiner, Appl. Phys. Lett. 60 (1992) 2484.

[8] R. Brunner, A. Bietsch, O. Hollricher, O. Marti, Rev. Sci. Instrum. 68 (1997) 1769.

[9] B. Hecht, H. Bielefeldt, Y. Inouye, D.W. Pohl, L. Novotny, J. Appl. Phys. 81 (1997) 2492.

[10] G.A. Valaskovic, M. Holton, G.H. Morrison, J. Micro. 179 (1995) 29.

[11] H. Heinzelmann, T. Huser, T. Lacoste, H.-J. Güntherodt, D.W. Pohl, B. Hecht, L. Novotny, O.J.F. Martin, Ch.V. Hafner, H. Baggenstos, U.P. Wild, A. Renn, Opt. Eng. 34 (1995) 2441.

[12] L. Novotny, D.W. Pohl, P. Regli, J. Opt. Soc. Am. A11 (1994) 1768.

[13] L. Novotny, D.W. Pohl, in: O. Marti, R. Möller (Eds.), Photons and Local Probes, Kluwer, Dordrecht, 1995, pp. 21–33.

[14] C. Serwatzy, M. Abraham, D. Drews, W. Ehrfeld, K. Mayr, W. Noell, O. Marti, O. Hollricher, P. Hahne, R. Ehmann, Numerical Simulations and Microfabrication of a Multifunctional AFM-SNOM-Sensor, PTB-Report F-30, 1997.